

## Water-Soluble Organometallic Compounds. 4. Catalytic Hydrogenation of Aldehydes in an Aqueous Two-Phase Solvent System Using a 1,3,5-Triaza-7-phosphaadamantane Complex of Ruthenium

Donald J. Darensbourg<sup>\*,1a</sup> Ferenc Joó,<sup>\*,1b</sup> Michael Kannisto,<sup>1a</sup> Agnes Kathó,<sup>1b</sup> Joseph H. Reibenspies,<sup>1a</sup> and Donald J. Daigle<sup>1c</sup>

Department of Chemistry, Texas A&M University, College Station, Texas 77843, Institute of Physical Chemistry, Kossuth Lajos University, Debrecen, H-4010 Hungary, and Southern Regional Research Center, U.S. Department of Agriculture, New Orleans, Louisiana 70179

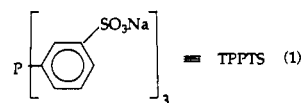
Received March 19, 1993\*

The water-soluble phosphine complex of ruthenium(II), *cis*-RuCl<sub>2</sub>(PTA)<sub>2</sub> (**3**), has been prepared by the reduction of RuCl<sub>3</sub> in ethanol in the presence of the air-stable phosphine 1,3,5-triaza-7-phosphaadamantane (**2**). Complex **3** is an effective catalyst for the regioselective conversion of unsaturated aldehydes to unsaturated alcohols using a biphasic aqueous/organic medium with sodium formate as the source of hydrogen, thus affording facile catalyst recovery and recycle. Both aromatic and aliphatic aldehydes were reduced to the corresponding alcohols. The formate ion was shown to directly be the hydrogen source by deuterium labeling experiments. The rate of hydrogenation of benzaldehyde was found to be first order in catalyst concentration, first order in substrate concentration (in the low-concentration regime), and independent of formate concentration at concentrations > 2.5 M. The reduction process was greatly retarded by the presence of excess phosphine ligand. The apparent activation energy determined was 23.9 kcal mol<sup>-1</sup>. A catalytic cycle was proposed which involves the rapid formation of a ruthenium hydride formate complex followed by phosphine dissociation and aldehyde addition in a slower step. Subsequent formation of a metal alkoxide intermediate and protonation completes the cycle. Recycling experiments demonstrated the catalyst to be quite robust. Complex **3** crystallized in the monoclinic system, space group *P*2<sub>1</sub>/*n*, with *a* = 11.399(7) Å, *b* = 19.281(8) Å, *c* = 15.068(7) Å, β = 110.85(4)°, *V* = 3095(3) Å<sup>3</sup>, and *D*<sub>calcd</sub> = 1.718 g cm<sup>-3</sup> for *Z* = 4 from a water solution. Complex **4**, RuCl<sub>2</sub>(PTA)<sub>2</sub>·2HCl, crystallized in the orthorhombic space group *Fdd*2, with *a* = 23.403(5) Å, *b* = 16.317(4) Å, *c* = 19.588(5) Å, *V* = 7480(3) Å<sup>3</sup>, and *D*<sub>calcd</sub> = 1.679 g cm<sup>-3</sup> for *Z* = 8 from a dilute HCl solution of **3**. In addition a small quantity of RuCl<sub>3</sub>(PTA)<sub>2</sub>·2HCl (**5**) crystallized in the triclinic space group *P* $\bar{1}$ , with *a* = 7.496(2) Å, *b* = 8.028(2) Å, *c* = 11.593(4) Å, α = 72.73(3)°, β = 72.98(2)°, γ = 78.08(2)°, *V* = 631.5(3) Å<sup>3</sup>, and *D*<sub>calcd</sub> = 1.753 g cm<sup>-3</sup> for *Z* = 1.

### Introduction

Catalyst recovery and recycle is an important concern for chemical processes homogeneously catalyzed by expensive transition metal complexes.<sup>2</sup> The application of metal catalysts in aqueous systems has recently received much attention, enabling an easy recovery of the catalyst by simple decantation.<sup>3</sup> It is extremely common for these transition metal catalysts to contain organophosphorus ligands.<sup>4</sup> Hence, a technique widely employed involves the use of sulfonated phosphines, namely Ph<sub>2</sub>P(*m*-C<sub>6</sub>H<sub>4</sub>-SO<sub>3</sub>Na) [TPPMS] and P(*m*-C<sub>6</sub>H<sub>4</sub>SO<sub>3</sub>Na)<sub>3</sub> [TPPTS] (**1**), which afford water-soluble complexes with metals. Owing to its higher solubility in water, **1** is generally the ligand of choice for carrying out commercial reactions in aqueous media and indeed has been incorporated into several important industrial processes, e.g., the

hydroformylation of propylene by RhCl(TPPTS)<sub>3</sub>,<sup>5</sup> the telomerization of dienes with Pd(TPPTS)<sub>4</sub>,<sup>6</sup> and the functionalization of dienes by *cis*-PtCl<sub>2</sub>(TPPTS)<sub>2</sub>.<sup>7</sup> It has been adequately demonstrated that the -SO<sub>3</sub><sup>-</sup> substituents have only a minor electronic influence on the nature of the metal-phosphorus bond.<sup>8–11</sup> However, there are significant steric differences between P(*m*-C<sub>6</sub>H<sub>4</sub>SO<sub>3</sub>Na)<sub>3</sub> and P(C<sub>6</sub>H<sub>5</sub>)<sub>3</sub>.<sup>11,12</sup>



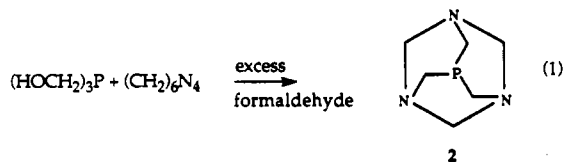
An alternative ligand under investigation in our laboratories, which is electronically and sterically quite different from TPPTS, yet is very water-soluble and air-stable, is the PTA ligand, 1,3,5-triaza-7-phosphaadamantane (**2**).<sup>13–16</sup> This tertiary phosphine

\* Abstract published in *Advance ACS Abstracts*, December 15, 1993.

- (1) (a) Texas A&M University. (b) Kossuth Lajos University. (c) U.S. Department of Agriculture.
- (2) (a) Andreetta, A.; Barberis, G.; Gregorio, G. *Chim. Ind. (Milan)* **1978**, *60*, 887. (b) Michalska, Z. M.; Webster, D. E. *Platinum Met. Rev.* **1974**, *18*, 65.
- (3) For reviews of this area, see: (a) Joó, F.; Tóth, Z. *J. Mol. Catal.* **1980**, *8*, 369. (b) Sinou, D. *Bull. Soc. Chim. Fr.* **1987**, 480. (c) Russell, M. J. H. *Platinum Met. Rev.* **1988**, *32*, 179. (d) Barton, M.; Atwood, J. D. *J. Coord. Chem.* **1991**, *24*, 43.
- (4) A noncomprehensive citing of various transformations catalyzed by water-soluble phosphines recently reported includes: (a) Fell, B.; Papadogiannakis, G. *J. Mol. Catal.* **1991**, *66*, 143. (b) Tóth, I.; Hanson, B. E.; Davis, M. E. *J. Organomet. Chem.* **1990**, *397*, 109. (c) Grosselin, J. M.; Mercier, C. *J. Mol. Catal.* **1990**, *63*, L25. (d) Casalnuovo, A. L.; Calabrese, J. C. *J. Am. Chem. Soc.* **1990**, *112*, 4324. (e) Peiffer, G.; Chhan, S.; Bendayan, A.; Waegell, B.; Zahra, J. *J. Mol. Catal.* **1990**, *59*, 1.

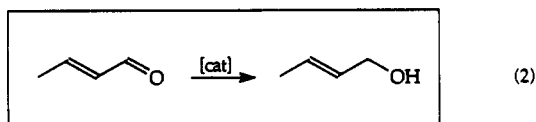
- (5) Kuntz, E. G. *CHEMTECH* **1987**, *17*, 570.
- (6) Kuntz, E. G. Fr. Patent 2366237, 1976.
- (7) Herrmann, W. A.; Kulpe, J. A.; Kellner, J.; Riepl, H.; Bahrman, H.; Konkol, W. *Angew. Chem., Int. Ed. Engl.* **1990**, *29*, 391.
- (8) Horváth, I.; Kastrop, R.; Oswald, A.; Mozeleski, E. *Catal. Lett.* **1989**, *2*, 85.
- (9) Herrmann, W. A.; Kellner, J.; Riepl, H. *J. Organomet. Chem.* **1990**, *389*, 103.
- (10) Larpent, C.; Patin, H. *Appl. Organomet. Chem.* **1987**, *1*, 529.
- (11) Darensbourg, D. J.; Bischoff, C. J.; Reibenspies, J. H. *Inorg. Chem.* **1991**, *30*, 1144.
- (12) Darensbourg, D. J.; Bischoff, C. J. *Inorg. Chem.* **1993**, *32*, 47.
- (13) Darensbourg, M. Y.; Daigle, D. *Inorg. Chem.* **1975**, *14*, 1217.
- (14) DeLerno, J. R.; Trefonas, L. M.; Darensbourg, M. Y.; Majeste, R. J. *Inorg. Chem.* **1976**, *15*, 816.

ligand is readily prepared from the reaction of formaldehyde, tris(hydroxymethyl)phosphine, and hexamethylenetetramine (eq 1) and is easily purified by recrystallization from ethanol.<sup>17</sup> It is



also noteworthy that the PTA ligand is not a pronounced surfactant, as are the sulfonated phosphines, thus providing better phase separations during catalysis in biphasic aqueous/organic media.

A process which has been the focus of observations of late is the selective hydrogenation of the aldehyde group in  $\alpha,\beta$ -unsaturated aldehydes employing Ru(II) TPPMS and TPPTS complexes as water-soluble catalysts (eq 2).<sup>18-20</sup> Indeed our entry



into the use of the PTA ligand in water-soluble biphasic catalysis has involved a study of this process.<sup>21</sup> Herein we wish to describe a full report of our research efforts on the highly selective catalytic reduction of the aldehyde functionality by ruthenium PTA complexes under biphasic conditions. Previous papers in this series are refs 11, 12, and 21.

## Experimental Section

**Reagents.** Analytical grade chlorobenzene, hydrogen, and carbon monoxide were obtained from Malinkrodt, Airco, and Trigas, respectively. D<sub>2</sub>O, acetone-*d*<sub>6</sub>, and sodium formate-*d* were purchased from Cambridge Isotope Laboratories. Sodium formate, barium chloride, sodium hydroxide, ruthenium(III) chloride trihydrate, silica gel (grade 62), ruthenium(IV) oxide, sodium periodate, and all other aldehydes were acquired from Aldrich and used without further purification. However, benzaldehyde, which was also obtained from Aldrich, was distilled prior to use. Water was distilled before using. Methylene chloride was procured from EM Science and was distilled over P<sub>2</sub>O<sub>5</sub>. Dowex 50W-X8 ion exchange resin and naphthalene were obtained from Baker, and hydrofluorosilicic acid was purchased from Pfaltz & Bauer. Benzyl alcohol and ethanol were acquired from MCB and Aaper, respectively.

**Instrumentation.** NMR spectra were collected on both Varian XL-200 (for <sup>13</sup>C and <sup>1</sup>H), and Varian XL-200E (<sup>31</sup>P) spectrometers. X-ray structure analyses were performed on a Nicolet R3m/v diffractometer employing Nicolet SHELXTL-PLUS and a Microvax II computer. Gas chromatographic analyses were made on a Chrom 5 gas chromatograph and a Perkin-Elmer 8500 gas chromatograph, both equipped with flame ionization detectors and with 6-ft long stainless steel columns packed with 3% OV-17 on Chrom-W. Mass spectral analyses were carried out employing a Hewlett-Packard 5995 gas chromatograph/mass spectrometer equipped with a 30-m capillary column packed with DB-5. pH measurements were performed with a Chemcadet pH meter Model 5986-60, equipped with a Cole-Parmer general-purpose glass electrode.

**Synthesis of Complexes.** *cis*-RuCl<sub>2</sub>(PTA)<sub>4</sub> (3). To a stirred, warm slurry of PTA (1.89 g, 12.0 mmol) in 50 mL 96% ethanol was added under nitrogen a warm solution of RuCl<sub>2</sub>·H<sub>2</sub>O (0.52 g, 2.0 mmol) in 25 mL of ethanol. The resulting mixture changed color in a few minutes from deep brown-red to light green-brown and was refluxed under nitrogen for 2 h. After the mixture was cooled to ambient temperature, the resultant solid was filtered and washed with ethanol and acetone. The product, RuCl<sub>2</sub>(PTA)<sub>4</sub>, was dried under vacuum to afford 1.6 g (98% yield) of a yellow powder. X-ray-quality crystals were obtained from a saturated water solution (<sup>1</sup>H NMR (200 MHz)  $\delta$  4.67 (broad singlet) and  $\delta$  4.40 (broad singlet)), which correspond to the methylene units between two nitrogens and between a nitrogen and a phosphorus, respectively. Concomitantly, the phosphines are all equivalent in the <sup>31</sup>P NMR spectrum, exhibiting a resonance at -47.3 ppm, as compared to -89.8 ppm in the free ligand. Anal. Calcd for C<sub>24</sub>H<sub>48</sub>N<sub>12</sub>P<sub>4</sub>Cl<sub>2</sub>Ru (*M*<sub>r</sub> 800.6): C, 36.01; H, 6.04; Cl, 8.86. Found: C, 35.95; H, 6.20; Cl, 8.88. A solution of 100 mg of RuCl<sub>2</sub>(PTA)<sub>4</sub> in 1.0 mL of 0.1 M HCl, when layered with 2.5 mL ethanol, afforded X-ray quality yellow crystals of *cis*-RuCl<sub>2</sub>(PTA)<sub>4</sub>·2HCl (4) containing four waters of hydration. Anal. Calcd for C<sub>24</sub>H<sub>58</sub>N<sub>12</sub>O<sub>4</sub>P<sub>4</sub>Cl<sub>4</sub>Ru (*M*<sub>r</sub> 945.58): C, 30.49; H, 6.18. Found: C, 32.55; H, 6.32. When the solution from which the yellow crystals were isolated was allowed to stand for several weeks, X-ray quality black crystals of RuCl<sub>3</sub>(PTA)<sub>2</sub>·2HCl (5) with four waters of hydration were obtained.

**Reactions of 3 with Carbon Monoxide.** Complex 3 (50 mg, 0.063 mmol) in 2.0 mL of 96% ethanol was stirred overnight at ambient temperature under an atmosphere of carbon monoxide. A yellow solid was isolated (6), which exhibited a strong  $\nu(\text{CO})$  infrared band at 1987 cm<sup>-1</sup> in KBr. Anal. Calcd for C<sub>19</sub>H<sub>36</sub>N<sub>9</sub>P<sub>3</sub>Cl<sub>2</sub>ORu: C, 33.99; H, 5.40. Found: C, 34.20; H, 5.70. The triphenylphosphine analog of this complex has previously been reported.<sup>22</sup>

**Kinetic Studies of the Catalytic Hydrogenation with Sodium Formate.** In a representative run, 5.0 mL of 5.0 M aqueous sodium formate solution, 24 mg (0.03 mmol) of RuCl<sub>2</sub>(PTA)<sub>4</sub>, 1.0 mL of 0.44 M naphthalene in chlorobenzene (internal standard), and 3.5 mL of chlorobenzene were charged into a thermostated (80 ± 1 °C) Schlenk flask equipped with a reflux condenser and a magnetic stirrer. A slow nitrogen flow was passed through the flask while this mixture was stirred for 10 min, followed by the addition of 0.5 mL (4.92 mmol) of benzaldehyde. Samples removed periodically from the organic phase were subjected to GC analysis. The concentration of benzyl alcohol was determined by calibrating its peak area against that of the naphthalene standard. Reduction of all other aldehydes was similarly followed by measuring percent conversion based on relative aldehyde and alcohol peak areas. In all cases, the reaction mixture was stirred at 2400 rpm.

In separate experiments, a flask was loaded with 5.0 mg (0.0625 mmol) of RuCl<sub>2</sub>(PTA)<sub>4</sub>, 0.5 mL (4.92 mmol) of benzaldehyde, 5.0 mL of 5.0 M aqueous sodium formate solution, and 5.0 mL of chlorobenzene all at once. After purging with nitrogen, the flask was pressurized with 1 atm of carbon monoxide or 10 equiv of PTA was added, heated to 80 °C, and stirred. After 3 h, an aliquot of the organic layer was removed, and subjected to GC analysis to determine percent aldehyde to alcohol conversion.

**Catalytic Hydrogenation with Hydrogen.** Into a 10-mL mini stainless steel reactor were introduced 50 mg (0.0625 mmol) of RuCl<sub>2</sub>(PTA)<sub>4</sub>, 2.5 mL of aqueous phosphate buffer (pH = 8), 2.5 mL of chlorobenzene, and 0.5 mL of benzaldehyde. After being heated to 80 °C, the reactor was pressurized to 400 psi with hydrogen, and the mixture was stirred for 5 h. When the reactor was cooled to ambient temperature and the remaining gas was vented, analysis of the organic phase showed a 46% conversion to benzyl alcohol.

**Labeling Experiments.** Into a 50-mL Schlenk flask was introduced 1.7 g (25 mmol) of sodium formate or sodium formate-*d* in 5.0 mL of H<sub>2</sub>O or D<sub>2</sub>O. This mixture was then stirred under a slow stream of nitrogen until all the salt had dissolved. To the flask was then added 36 mg (0.045 mmol) of RuCl<sub>2</sub>(PTA)<sub>4</sub> and 4.5 mL of chlorobenzene. This mixture was heated to 90 °C and stirred for 10 min, at which time 0.5 mL (4.9 mmol) of benzaldehyde was added and the mixture again stirred under nitrogen. After 5 h, the solution was cooled, 10 mL of distilled water was added, and the organic phase was removed. Onto a 30 cm × 1.5 cm column of silica gel was placed a 2.0-mL aliquot of the organic phase, which was eluted with methylene chloride. The fraction containing only benzyl alcohol (as identified by GC) was heated to 40 °C to evaporate

- (15) Fluck, E.; Förster, J. E.; Weidlein, J.; Hädicke, E. *Z. Naturforsch.* **1977**, *32B*, 499.  
 (16) Fisher, K. J.; Alyea, E. C.; Shahnazarian, N. *Phosphorus, Sulfur, Silicon Relat. Elem.* **1990**, *48*, 37.  
 (17) (a) In the initial publication this ligand was referred to as PAA as opposed to PTA. (b) Daigle, D. J.; Peppermann, A. B., Jr.; Vail, S. L. *J. Heterocycl. Chem.* **1974**, *17*, 407.  
 (18) Joó, F.; Benyei, A. *J. Organomet. Chem.* **1989**, *363*, C19.  
 (19) Benyei, A.; Joó, F. *J. Mol. Catal.* **1990**, *58*, 151.  
 (20) Grosselin, J. M.; Mercier, C.; Allmang, G.; Grass, F. *Organometallics* **1991**, *10*, 2126.  
 (21) Darensbourg, D. J.; Joó, F.; Kannisto, M.; Kathó, A.; and Reibenspies, J. H. *Organometallics* **1992**, *11*, 1990.

- (22) (a) Halpern, J.; James, B. R.; Kemp, A. L. *W. J. Am. Chem. Soc.* **1966**, *88*, 5142. (b) Poddar, R. K.; Agarwala, U. *Indian J. Chem.* **1971**, *9*, 477.

Table 1. Crystallographic Data for Complexes 3–5

	3	4	5
(a) Crystal Data			
formula	C <sub>24</sub> H <sub>48</sub> N <sub>12</sub> P <sub>4</sub> Cl <sub>2</sub> Ru	C <sub>24</sub> H <sub>58</sub> N <sub>12</sub> O <sub>4</sub> P <sub>4</sub> Cl <sub>4</sub> Ru	C <sub>12</sub> H <sub>34</sub> N <sub>6</sub> O <sub>4</sub> P <sub>2</sub> Cl <sub>3</sub> Ru
fw	800.6	945.6	666.7
cryst syst	monoclinic	orthorhombic	triclinic
space group	<i>P</i> 2 <sub>1</sub> / <i>n</i> (No. 14)	<i>F</i> dd2	<i>P</i> 1̄ (No. 2)
<i>a</i> , Å	11.399(7)	23.403(5)	7.496(2)
<i>b</i> , Å	19.281(8)	16.317(4)	8.028(2)
<i>c</i> , Å	15.068(7)	19.588(5)	11.593(4)
$\alpha$ , deg			72.73(3)
$\beta$ , deg	110.85(4)		72.98(2)
$\gamma$ , deg			78.08(2)
<i>V</i> , Å <sup>3</sup>	3095(3)	7480(3)	631.5(3)
<i>Z</i>	4	8	1
<i>D</i> <sub>calcd</sub> , g/mL	1.718	1.679	1.753
temp, K	193	193	193
cryst dims, mm	0.10 × 0.21 × 0.48	0.28 × 0.30 × 0.34	0.08 × 0.20 × 0.24
$\mu$ (Mo K $\alpha$ ), mm <sup>-1</sup>	0.915	0.917	1.298
(b) Data Collection			
radiation	Mo K $\alpha$	Mo K $\alpha$	Mo K $\alpha$
wavelength, Å	0.710 73	0.710 73	0.710 73
no. of rflns colld	5860	1811	2347
no. of unique rflns	4403	1668	1978
(c) Refinement			
<i>R</i>	0.048	0.025	0.056
<i>R</i> <sub>w</sub>	0.055	0.030	0.064
<i>S</i>	2.03	2.39	3.42

the solvent, and the alcohol remaining was dissolved in 0.5 mL of acetone-*d*. Several microliters of this sample were then analyzed by GC/mass spectrometry to observe changes around the *m/e* 79 and 108 signals characteristic of pure benzyl alcohol. The remainder of the sample was analyzed by <sup>13</sup>C{<sup>1</sup>H} NMR (200 pulses at a width of 5  $\mu$ s; pulse repetition time, 20 s).

**Preparation of [Ru(H<sub>2</sub>O)<sub>6</sub>][Tos]<sub>2</sub> and Its Use as a Catalyst.** [Ru(H<sub>2</sub>O)<sub>6</sub>][Tos]<sub>2</sub> was prepared as described by Bernhardt et al.<sup>23</sup> from ruthenium(IV) oxide, sodium periodate, and lead. Into a 50-mL Schlenk flask were placed 3.5 mL of chlorobenzene, 1.0 mL of naphthalene standard solution, 5.0 mL of 5 M aqueous sodium formate solution, 16.54 mg (0.03 mmol) of [Ru(H<sub>2</sub>O)<sub>6</sub>][Tos]<sub>2</sub>, and either 4.72 mg (0.03 mmol), 9.42 mg (0.06 mmol), 14.15 mg (0.09 mmol), 18.86 mg (0.12 mmol), or 28.29 mg (0.18 mmol) of free PTA. This mixture was then heated to 80 °C and stirred under a nitrogen stream for 10 min, at which time 0.5 mL (4.92 mmol) of benzaldehyde was added. As above, the appearance of benzyl alcohol was monitored in reference to the standard naphthalene peak in the GC spectrum.

**pH Dependence of Hydrogenation Reaction.** Into a 50-mL Schlenk flask were placed 5.0 mL of 5 M aqueous sodium formate solution, 5.0 mL of chlorobenzene, and 50 mg (0.060 mmol) of RuCl<sub>2</sub>(PTA)<sub>4</sub>. This mixture was then heated to 80 °C and stirred under a blanket of nitrogen for 10 min, at which time 0.5 mL of benzaldehyde was added. Periodically, the entire aqueous layer was transferred to a test tube, the pH was determined using a narrow glass electrode equipped with a thermocouple, and the aqueous layer was returned to the reaction flask.

**Catalyst Recycling Experiments.** Into a 50-mL Schlenk flask were placed 5.0 mL of 5 M sodium formate solution, 5.0 mL of chlorobenzene, and 52.3 mg (0.065 mmol) of RuCl<sub>2</sub>(PTA)<sub>4</sub>. This mixture was then heated to 80 °C and stirred under a blanket of nitrogen for 10 min, at which time 0.5 mL benzaldehyde was added. The mixture was allowed to stir for 4 h at 80 °C and then overnight at ambient temperature. The following morning the organic layer was removed, replaced with fresh chlorobenzene and benzaldehyde, and allowed to react again at 80 °C and overnight at ambient temperature. After three such cycles, the aqueous layer had become clouded with a white sticky, powdery residue, which was found to contain sodium formate, sodium carbonate, and sodium bicarbonate. Analysis was performed both on samples just as they came out of the reaction vessel and on samples after washing with acetone and methanol and drying in vacuo. Carbonate and bicarbonate composition were determined using a procedure described by Harris,<sup>24</sup> involving titration of a sample to determine total alkalinity, converting all bicarbonate to carbonate in a separate sample with NaOH solution,

complexing carbonate with barium chloride, and back-titrating excess hydroxide to determine bicarbonate concentration. Samples of 1:1:1 sodium carbonate, sodium bicarbonate, and sodium formate were also analyzed to insure formate does not interfere with this analytical technique.

**X-ray Structural Determinations.** A pale yellow parallelepiped (0.28 mm × 0.30 mm × 0.34 mm) of complex 3 was mounted on a glass fiber with epoxy cement at room temperature and cooled to 193 K in a N<sub>2</sub> cold stream (Nicolet LT-2). Data collection was performed on a Nicolet R3m/V X-ray diffractometer in the range 5.0° ≤ 2 $\theta$  ≤ 50.0°. Lorentz and polarization corrections were applied to a total of 1811 reflections collected, of which 1668 were unique with *I* ≥ 1.3 $\sigma$ (*I*).

A yellow needle (0.10 mm × 0.21 mm × 0.48 mm) of complex 4 was mounted on a glass fiber with epoxy cement at room temperature and cooled to 193 K in a N<sub>2</sub> cold stream (Nicolet LT-2). Data collection was performed on a Nicolet R3m/V X-ray diffractometer in the range 5.0° ≤ 2 $\theta$  ≤ 50.0°. Lorentz and polarization corrections were applied to a total of 5860 reflections collected, of which 4403 were unique with *I* ≤ 2.0 $\sigma$ (*I*).

Similarly a red-brown plate (0.08 mm × 0.20 × 0.24 mm) of complex 5 was mounted on a glass fiber with epoxy cement at room temperature and cooled to 193 K in a N<sub>2</sub> cold stream (Nicolet LT-2). Data collection was performed on a Nicolet R3m/V X-ray diffractometer in the range 4.0° ≤ 2 $\theta$  ≤ 50.0°. Lorentz and polarization corrections were applied to a total of 2347 reflections, of which 1978 were unique with *I* ≥ 2.0 $\sigma$ (*I*).

All three structures were solved by Patterson synthesis (SHELXS, SHELXTL-PLUS program package of Sheldrick). Pertinent crystallographic parameters for the three structures are listed in Table 1.

## Results and Discussion

**Synthesis.** The ruthenium complex of interest, RuCl<sub>2</sub>(PTA)<sub>4</sub> (3), was prepared by the reaction of hydrated ruthenium trichloride with 6 equiv of PTA in refluxing ethanol. The yellow complex precipitated from solution in nearly quantitative yield. Optionally complex 3 can be obtained by extracting toluene or dichloromethane solutions of RuCl<sub>2</sub>(PPh<sub>3</sub>)<sub>3</sub> with an aqueous solution of PTA (2). It is important to note that 2 is highly soluble in water to the extent of 1.5 M. Complex 3 is soluble in alkaline or neutral aqueous solutions (>0.1 M) but is only sparingly soluble in ethanol and 2-methoxyethanol and is insoluble in nonpolar organic solvents. When the extraction is done with a 0.1 M HCl solution of 2, or 3 is recrystallized from dilute HCl, the diprotonated product [RuCl<sub>2</sub>(PTA)<sub>2</sub>(PTAH)<sub>2</sub>]Cl<sub>2</sub> (4) is obtained. In addition a small quantity of shiny black crystals

(23) Bernhardt, P.; Biner, M.; Ludi, A. *Polyhedron* 1990, 9, 1095.

(24) Harris, D. C. *Quantitative Chemical Analysis*, 2nd ed.; W. H. Freeman and Co.: New York, 1987; p 685.

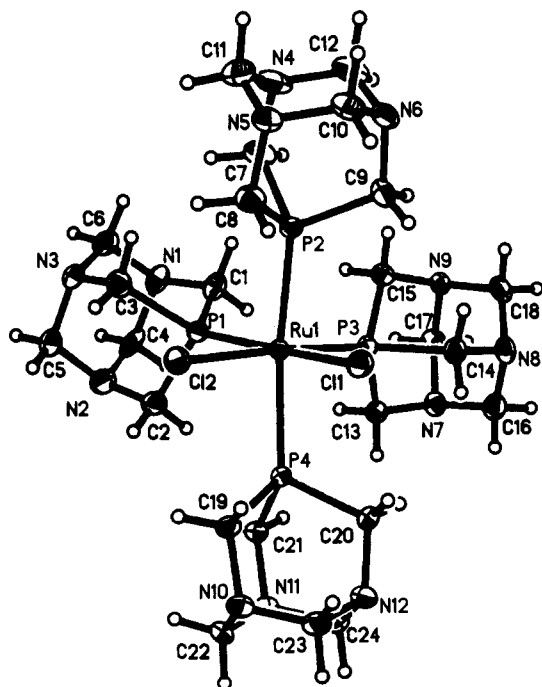
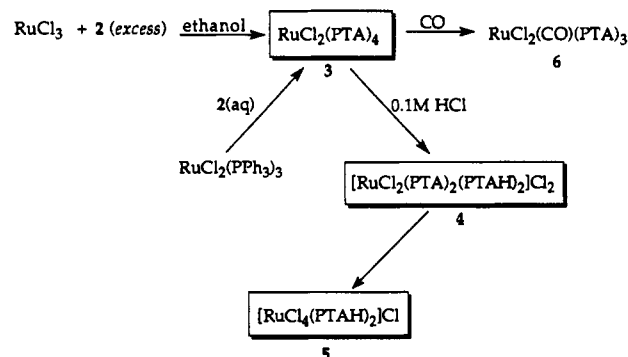


Figure 1. ORTEP diagram of  $\text{RuCl}_2(\text{PTA})_4$  (**3**) with atom numbering scheme showing 50% probability thermal ellipsoids.

#### Scheme 1



were obtained which analyzed to be the Ru(III) species  $[\text{RuCl}_4(\text{PTAH})_2]\text{Cl}$  (**5**). This latter complex was shown to be produced by two processes; adventitious air oxidation of complex **4** during prolonged crystal growing experiments and incomplete reduction of Ru(III) at the time of the initial synthesis of complexes **3** and **4**. Displacement of a PTA ligand in **3** by carbon monoxide at ambient temperature in 2-methoxyethanol afforded the derivative,  $\text{RuCl}_2(\text{CO})(\text{PTA})_3$  (**6**). Complex **6** exhibited a  $\nu(\text{CO})$  infrared band at  $1987\text{ cm}^{-1}$  in KBr. These reactions are summarized in Scheme 1.

**Structure of Complex 3.** Single-crystal X-ray crystallography of **3** showed the structure to consist of well-separated molecular units. **3** crystallized in the  $P2_1/n$  space group and its structure is depicted in Figure 1. Final atomic positional parameters for the non-hydrogen atoms are provided in Table 2. Selected bond distances and bond angles are listed in Table 3.

Four equivalent molecules were observed in the monoclinic unit cell. Each ruthenium atom possesses a distorted octahedral geometry with *cis* chloride ligands. The two axial Ru-P bond lengths are longer than the two equatorial Ru-P bond lengths which are *trans* to chloride ligands. These Ru-P distances are  $2.370[2]$  and  $2.260[2]$  Å, respectively. The two Ru-Cl bond lengths have an average value of  $2.496[2]$  Å with a  $\angle\text{Cl}-\text{Ru}-\text{Cl}$  of  $84.2(1)$ . It is of note to point out that all of the N-C distances in the four PTA ligands in **3** are quite similar, displaying a range of values of  $1.450(9)$ – $1.485(9)$  Å with an average value of  $1.467$ -

Table 2. Atomic Coordinates ( $\times 10^4$ ) and Equivalent Isotropic Displacement Parameters ( $\text{\AA}^2 \times 10^3$ ) for Compound **3**

	x	y	z	$U(\text{eq})^{a,b}$
Ru1	2052(1)	8127(1)	9015(1)	15(1)
Cl1	-258(1)	8303(1)	8491(1)	23(1)
Cl2	1506(1)	7333(1)	7611(1)	23(1)
P1	4084(1)	7905(1)	9220(1)	18(1)
P2	1904(1)	9086(1)	8018(1)	18(1)
P3	2443(1)	8808(1)	10303(1)	17(1)
P4	1612(1)	7159(1)	9836(1)	17(1)
N1	6621(4)	8268(3)	9837(3)	27(2)
N2	6163(5)	7016(3)	9842(4)	31(2)
N3	5777(5)	7622(3)	8326(3)	25(2)
N4	2684(5)	10125(3)	7084(5)	41(2)
N5	729(5)	9516(3)	6152(4)	31(2)
N6	734(5)	10357(2)	7381(3)	26(2)
N7	3235(5)	8954(2)	12271(3)	22(2)
N8	1381(4)	9644(2)	11312(3)	22(2)
N9	3508(4)	9983(2)	11390(3)	20(2)
N10	424(5)	5875(2)	9644(3)	24(2)
N11	2117(5)	6096(2)	11178(3)	22(2)
N12	84(5)	6684(2)	10789(3)	26(2)
C1	5401(5)	8504(3)	9843(4)	24(2)
C2	4869(6)	7109(3)	9839(5)	28(2)
C3	4449(5)	7771(3)	8125(4)	26(2)
C4	6967(6)	7594(3)	10326(5)	33(2)
C5	6140(6)	6974(3)	8861(4)	29(2)
C6	6575(5)	8186(3)	8863(4)	27(2)
C7	3175(6)	9588(3)	7821(5)	34(3)
C8	995(6)	8897(3)	6765(4)	27(2)
C9	972(6)	9840(3)	8154(4)	28(2)
C10	21(6)	10041(3)	6457(4)	32(2)
C11	1895(7)	9821(4)	6171(5)	44(3)
C12	1911(6)	10638(3)	7363(5)	35(3)
C13	3164(5)	8448(3)	11527(4)	20(2)
C14	1064(5)	9226(3)	10445(4)	22(2)
C15	3446(6)	9602(3)	10529(4)	23(2)
C16	1986(6)	9219(3)	12158(4)	25(2)
C17	4025(6)	9542(3)	12235(4)	26(2)
C18	2241(5)	10207(3)	11318(4)	25(2)
C19	818(5)	6406(3)	9103(4)	22(2)
C20	418(6)	7319(3)	10392(4)	26(2)
C21	2737(5)	6646(3)	10819(4)	20(2)
C22	1500(6)	5598(3)	10426(4)	24(2)
C23	-451(6)	6168(3)	10043(5)	27(2)
C24	1182(6)	6391(3)	11525(4)	26(2)

<sup>a</sup> Equivalent isotropic  $U$  defined as one-third of the trace of the orthogonalized  $U_{ij}$  tensor. <sup>b</sup> Estimated standard deviations are given in parentheses.

Table 3. Selected Interatomic Distances (Å) and Angles (deg) for Compound **3**<sup>a</sup>

Bond Distances			
Ru1-Cl1	2.488(2)	Ru1-Cl2	2.503(2)
Ru1-P1	2.267(2)	Ru1-P2	2.351(2)
Ru1-P3	2.252(2)	Ru1-P4	2.388(2)
Bond Angles			
Cl1-Ru1-Cl2	84.2(1)	Cl1-Ru1-P1	169.7(1)
Cl2-Ru1-P1	86.2(1)	Cl1-Ru1-P2	82.1(1)
Cl2-Ru1-P2	90.0(1)	P1-Ru1-P2	94.2(1)
Cl1-Ru1-P3	93.3(1)	Cl2-Ru1-P3	176.3(1)
P1-Ru1-P3	96.5(1)	P2-Ru1-P3	92.2(1)
Cl1-Ru1-P4	83.0(1)	Cl2-Ru1-P4	85.7(1)
P1-Ru1-P4	100.1(1)	P2-Ru1-P4	164.8(1)
P3-Ru1-P4	91.3(1)		

<sup>a</sup> Estimated standard deviations are given in parentheses.

[8] Å. Other intraligand distances which are alike are the P-C distances which span a range of  $1.837(5)$ – $1.868(6)$  Å with an average value of  $1.856[7]$  Å. These intraligand bond distances are essentially the same as those noted in the free PTA ligand, where the P-C bond length is  $1.857(3)$  Å and the N-C bond distances have a spread of  $1.461(4)$ – $1.465(4)$  Å.<sup>15</sup>

**Structure of Complex 4.** The molecular structure of complex **4** was established by a single-crystal X-ray diffraction analysis. An ORTEP drawing of the molecular structure of **4** is shown in

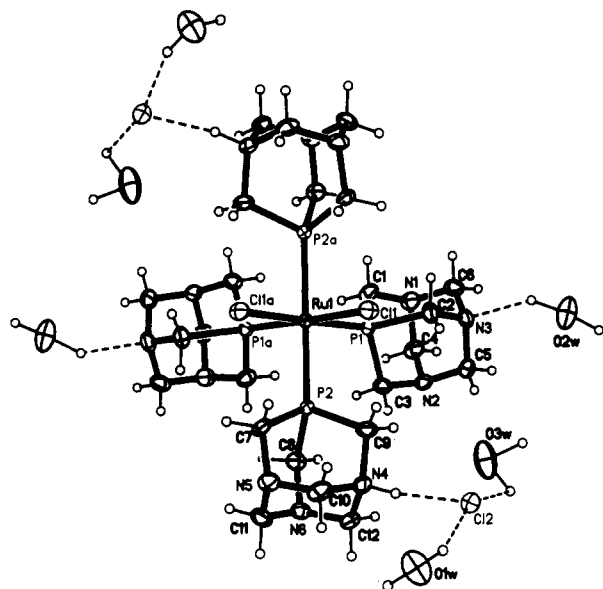


Figure 2. ORTEP diagram of  $\text{RuCl}_2(\text{PTA})_4 \cdot 2\text{HCl}$  (**4**) with atom numbering scheme showing 50% probability thermal ellipsoids.

Table 4. Atomic Coordinates ( $\times 10^4$ ) and Equivalent Isotropic Displacement Parameters ( $\text{\AA}^2 \times 10^3$ ) for Compound **4**

	<i>x</i>	<i>y</i>	<i>z</i>	<i>U</i> (eq) <sup>a,b</sup>
Ru1	0	0	0	13(1)
Cl1	602(1)	-556(1)	-917(1)	24(1)
P1	609(1)	-566(1)	779(1)	16(1)
P2	557(1)	1201(1)	-178(1)	15(1)
C1	348(2)	-1199(3)	1502(3)	25(2)
C2	1149(2)	-1291(3)	444(3)	25(2)
C3	1107(2)	72(3)	1284(3)	22(2)
N1	814(2)	-1543(3)	1917(3)	27(1)
C4	1164(2)	-891(3)	2224(3)	27(2)
N2	1490(2)	-419(3)	1723(3)	22(1)
C5	1851(2)	-968(3)	1312(3)	27(2)
N3	1524(2)	-1629(3)	975(3)	26(1)
C6	1193(2)	-2075(3)	1499(3)	30(2)
C7	294(2)	1906(3)	-851(3)	21(2)
C8	757(2)	1999(3)	447(3)	23(2)
C9	1279(2)	1017(3)	-538(3)	25(2)
n4	1568(2)	1807(3)	-730(2)	22(1)
C10	1226(2)	2275(3)	-1271(3)	28(2)
N5	697(2)	2573(3)	-997(3)	27(1)
C11	809(2)	3091(3)	-404(3)	28(2)
N6	1116(2)	2657(2)	142(2)	23(1)
C12	1657(2)	2360(3)	-115(3)	23(1)
O1W	0	0	4885(4)	50(2)
O2W	0	0	2883(3)	48(2)
O3W	-85(2)	2845(3)	2535(3)	58(2)
Cl2	2650(1)	1189(1)	-1427(1)	28(1)

<sup>a</sup> Equivalent isotropic *U* defined as one-third of the trace of the orthogonalized  $U_{ij}$  tensor. <sup>b</sup> Estimated standard deviations are given in parentheses.

Figure 2. Final atomic positional parameters are listed in Table 4. Selected interatomic distances and angles are listed in Table 5. The molecule consists of a distorted octahedral geometry with cis chloride ligands much like that seen in complex **3**. The major difference between complexes **3** and **4** is that the two mutually trans phosphine ligands are protonated at one of nitrogen atoms in complex **4**. These quaternary nitrogens possess N–C average bond distances, 1.578[7] Å, slightly longer than their tertiary counterparts in the same ligand, 1.461[7] Å, or in the neutral PTA ligands in **4**, 1.474[7] Å. Similarly, the N–C bond lengths in **3** exhibit an average value of 1.467[8] Å (vide supra).

The free chloride ions in complex **4** are hydrogen-bonded to the protonated nitrogen atoms, with a N–H...Cl distance of 3.050 Å being observed. These chloride ions are each additionally solvated by two water molecules. Furthermore, one nitrogen atom

Table 5. Selected Interatomic Distances (Å) and Angles (deg) for Compound **4**<sup>a</sup>

Bond Distances			
Ru1–Cl1	2.457(2)	Ru1–P1	2.282(2)
Ru1–P2	2.379(1)		
Bond Angles			
Cl1–Ru1–P1	89.0(1)	P2–Ru1–P2A	163.1(1)
P1–Ru1–P2	95.1(1)	Cl1–Ru1–P2	83.3(1)
P1–Ru1–Cl1A	175.0(1)	Cl1–Ru1–Cl1A	86.0(1)
P2–Ru1–P1A	96.1(1)	P1–Ru1–P1A	96.1(1)
Cl1–Ru1–P2A	84.4(1)		

<sup>a</sup> Estimated standard deviations are given in parentheses.

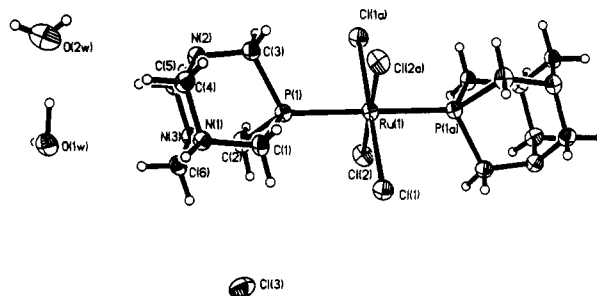


Figure 3. ORTEP diagram of  $\text{RuCl}_3(\text{PTA})_2 \cdot 2\text{HCl}$  (**5**) with atom numbering scheme showing 50% probability thermal ellipsoids.

Table 6. Atomic Coordinates ( $\times 10^4$ ) and Equivalent Isotropic Displacement Parameters ( $\text{\AA}^2 \times 10^3$ ) for Compound **5**

	<i>x</i>	<i>y</i>	<i>z</i>	<i>U</i> (eq) <sup>a,b</sup>
Ru1	0	0	0	17(1)
Cl1	2331(2)	-98(2)	1034(2)	27(1)
Cl2	-543(2)	-2881(2)	1186(2)	28(1)
Cl3	0	0	5000	40(1)
P1	-2327(2)	1310(2)	1431(2)	18(1)
O1W	-7806(7)	4709(6)	5628(5)	33(2)
O2W	-9031(9)	7073(7)	3656(5)	51(3)
N1	-3105(7)	3561(7)	2956(5)	20(2)
N2	-5459(7)	3780(7)	1800(5)	22(2)
N3	-5149(7)	1261(7)	3574(5)	22(2)
C1	-1482(9)	2684(8)	2130(6)	22(2)
C2	-3818(9)	56(8)	2864(6)	25(3)
C3	-4173(9)	2926(8)	840(6)	23(3)
C4	-4484(10)	4764(8)	2221(6)	26(3)
C5	-6411(9)	2476(8)	2870(6)	23(3)
C6	-4178(9)	2215(9)	4026(6)	23(3)

<sup>a</sup> Equivalent isotropic *U* defined as one-third of the trace of the orthogonalized  $U_{ij}$  tensor. <sup>b</sup> Estimated standard deviations are given in parentheses.

from each of the nonprotonated PTA ligands is hydrogen-bonded to a water molecule with a N...H–O bond distance of 2.930 Å. As in complex **3** the two mutually trans Ru–P bond lengths are longer by 0.097 Å, 2.379(1) vs 2.282(1) Å. The Ru–Cl bond distances are 2.457(2) Å, with a  $\angle\text{Cl–Ru–Cl}$  of 86.0(1)°. Hence, the coordination geometry about the Ru(II) center is not significantly affected by protonation of the PTA ligands.

**Structure of Complex 5.** Details of the metal coordination environment in complex **5** were revealed in a single-crystal X-ray structure determination. **5** crystallizes in the triclinic space group  $P\bar{1}$  and an ORTEP drawing of its molecular structure is depicted in Figure 3, together with the atomic labeling system. Final atomic positional parameters for the non-hydrogen atoms are provided in Table 6. Selected bond lengths and angles are listed in Table 7.

The molecular structure of **5** consists of an octahedral arrangement of four chloride and two PTA ligands in a trans configuration. One nitrogen atom in each of the PTA ligands is protonated. This is evident by the N–C distances; i.e., the three N(1)–C distances average 1.520[8] Å whereas the other six tertiary N–C bond lengths average 1.462[8] Å. In addition there is one chloride ion, along with four water molecules, which are

**Table 7.** Selected Interatomic Distances (Å) and Angles (deg) for Compound 5<sup>a</sup>

Bond Distances			
Ru1–Cl1	2.369(2)	Ru1–Cl2	2.362(2)
Ru1–P1	2.342(2)		
Bond Angles			
Cl1–Ru1–Cl2	90.0(1)	P1–Ru1–P1A	180.0(1)
Cl1–Ru1–P1	93.2(1)	Cl1–Ru1–P1A	91.7(1)
Cl2–Ru1–Cl1A	90.0(1)	Cl1–Ru1–Cl1A	180.0(1)
P1–Ru1–Cl2A	86.8(1)	Cl2–Ru1–Cl2A	180.0(1)
Cl1–Ru1–P1A	88.3(1)		

<sup>a</sup> Estimated standard deviations are given in parentheses.

**Table 8.** Catalytic Hydrogenation of Various Aldehydes to the Corresponding Alcohols by Complex 3<sup>a</sup>

substrate (amount, mmol)	conversion, % <sup>b</sup>
benzaldehyde (4.92)	64.0 <sup>c</sup> 0.40 <sup>d</sup> 7.1 <sup>e</sup>
4-methylbenzaldehyde (4.24)	23.6
4-methoxybenzaldehyde (4.11)	26.7
4-bromobenzaldehyde (1.35)	16.3
2-hydroxybenzaldehyde (4.69)	0.0
2-butenal (6.04)	87.6
3-phenyl-2-propenal (3.96)	21.2
propanal (6.93)	81.6
butanal (5.55)	72.8
pentanal (4.70)	46.1
hexanal (4.16)	23.0

<sup>a</sup> Conditions: 0.0625 mmol of 3, 5 mL of chlorobenzene and 5 mL of 5 M HCO<sub>2</sub>Na in water; 80 °C; reaction time 3 h. <sup>b</sup> By GC analysis. <sup>c</sup> Under the same catalytic conditions in the presence of 1 atom of H<sub>2</sub>, a 2.6% conversion was achieved. However, under 400 psi of H<sub>2</sub>, a 45.9% conversion was noted in 5 h for a phosphate-buffered reaction mixture (pH = 8). <sup>d</sup> Reaction carried out in the presence of a 10-fold excess of PTA. <sup>e</sup> Reaction carried out in the presence of an atmosphere of CO.

not in the metal's coordination sphere. The Ru–P and Ru–Cl distances of 2.342(2) and 2.366[2] Å respectively, are consistent with a Ru<sup>3+</sup> metal center.

**Biphasic Homogeneous Catalysis.** The water-soluble ruthenium PTA complex 3 is an effective catalyst for the conversion of aldehydes to alcohols using a biphasic aqueous-organic medium with sodium formate as a source of hydrogen.<sup>25,26</sup> Table 8 illustrates the range of aldehydes investigated, along with their percent conversion to alcohols for a given quantity of substrate after 3 h at 80 °C in the presence of 0.0625 mmol of 3 (e.g., for benzaldehyde as substrate the catalytic activity was observed to be 16.8 turnovers/(metal/h)). As is evident in Table 8 aliphatic aldehydes are reduced more slowly as the hydrocarbon chain length increases. The reaction is greater than 98% selective toward carbonyl reduction as illustrated by the high regioselectivity exhibited by 2-butenal (crotonaldehyde) and 3-phenyl-2-propenal (cinnamaldehyde), where only the corresponding crotyl and cinnamyl alcohols are produced. Indeed, the selectivity of complex 3 toward aldehyde reduction is so pronounced that it was not possible to reduce 1-decene at all employing 3 as catalyst. By way of contrast, the analogously performed hydrogenation process using the rhodium catalyst, RhCl(PTA)<sub>3</sub>, selectively hydrogenated cinnamaldehyde to 3-phenylpropionaldehyde (dihydrocinnamaldehyde) at an enhanced initial rate (i.e., the turnover frequency at 50 °C was found to be 82 h<sup>-1</sup>).<sup>21</sup>

**Kinetics of Benzaldehyde Hydrogenation Using Sodium Formate as Hydrogen Source.** Obtaining reliable kinetic data for reactions performed in biphasic media is often complicated by various physical phenomena. For example, it is necessary to employ very high stirring rates (>2000 rpm) to ensure rapid mass transfer

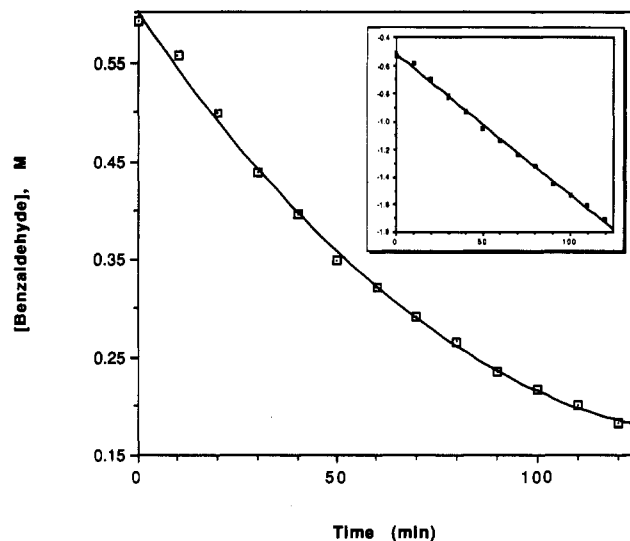
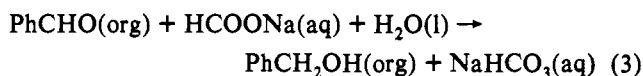


**Figure 4.** Rate data for the catalytic hydrogenation of benzaldehyde. Conditions: 0.03 mmol of RuCl<sub>2</sub>(PTA)<sub>4</sub> in 5.0 mL of 5 M aqueous sodium formate, 2.95 mmol of benzaldehyde in 3.7 mL chlorobenzene; 80 °C. Inset shows linearity of plot of ln [benzaldehyde] vs time, which provides a pseudo-first-order rate constant of 1.01 × 10<sup>-2</sup> min<sup>-1</sup>.

between gas-liquid and/or organic-aqueous phases.<sup>27</sup> An accompanying difficulty associated with substrate diffusion between the aqueous and organic phases is the generally low solubility of the substrate in the aqueous phase. In order to overcome these problems we focused our attention on the hydrogenation of benzaldehyde, a substrate with sufficient solubility in the aqueous phase,<sup>28</sup> with the very water soluble hydrogen source sodium formate. In addition, a high stirring rate of 2400 rpm was maintained in our studies in an effort to assure that the aforementioned physical phenomena were not rate determining. It has previously been demonstrated for the closely related, and identically performed, studies involving RuCl<sub>2</sub>(TPPMS)<sub>2</sub> that the aldehyde reduction rate was independent of the stirring rate in the 500–1250 rpm range as measured with a stroboscope.<sup>19</sup> Hence, the reaction rates were assumed to be determined by the chemical aspects governing these catalytic processes.

The aqueous/chlorobenzene catalyst mixture of RuCl<sub>2</sub>(PTA)<sub>4</sub> and sodium formate were thermostated at 80 °C under a nitrogen atmosphere with stirring for 10 min prior to introduction of the substrate, benzaldehyde. This systematic catalyst pretreatment led to highly reproducible rate data for hydrogenation which exhibited no induction period. A typical hydrogenation profile is shown in Figure 4 for the reduction of benzaldehyde to benzyl alcohol (eq 3) under the conditions indicated in Table 8. As is



apparent from Figure 4 the decay of substrate is exponential for at least two-thirds of the reaction.

In an attempt to elucidate the reaction pathway of the catalytic process in some detail, the effect of the concentrations of the catalyst, aldehyde, and sodium formate on the initial rate of hydrogenation of benzaldehyde was investigated. The results of these rate studies are illustrated in Figures 5–7. As indicated in Figure 5 the reaction is first-order with respect to the concentration of the catalyst precursor, complex 3. On the other hand the rate of the reaction as a function of benzaldehyde concentration initially exhibited an increase, ultimately reaching a maximum at a benzaldehyde concentration of 3.5 M (>60% by volume of the organic phase), after which the rate decreased (Figure 6).

(25) Other reports of aldehyde reductions using formate as a source of hydrogen in biphasic or phase transfer processes include refs 18, 19, and 26.

(26) (a) Tsuji, J.; Yamakawa, T. *Tetrahedron Lett.* 1979, 613. (b) Bar, R.; Sasson Y.; Blum, J. *J. Mol. Catal.* 1984, 26, 327.

(27) Bar, R.; Bar, L. K.; Sasson, Y.; Blum, J. *J. Mol. Catal.* 1985, 33, 161.

(28) Benzaldehyde is soluble in 350 parts water at ambient temperature.

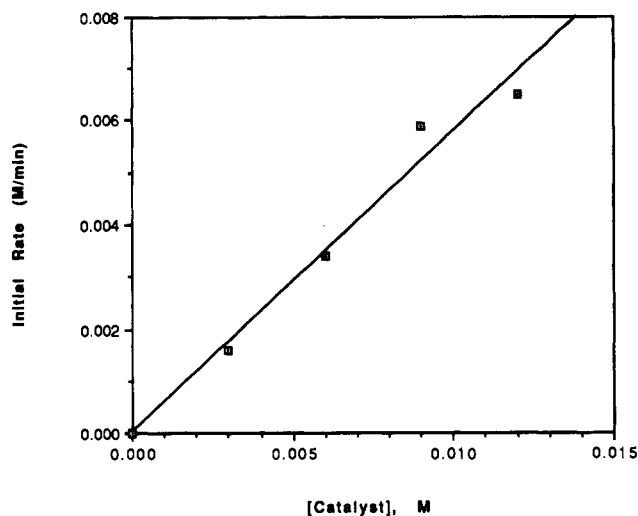


**Figure 5.** Dependence of the initial rate on the catalyst concentration. Conditions:  $\text{RuCl}_2(\text{PTA})_4$  (0–0.06 mmol) in 5.0 mL of 5 M aqueous sodium formate; 4.92 mmol of benzaldehyde in 3.5 mL of chlorobenzene; 80 °C.

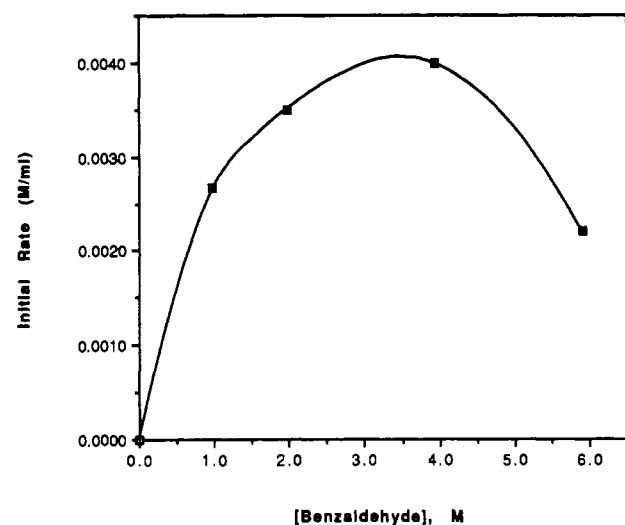


**Figure 6.** Dependence of the initial rate on the concentration of benzaldehyde. Conditions: 0.03 mmol  $\text{RuCl}_2(\text{PTA})_4$  in 5.0 mL of 5 M aqueous sodium formate; benzaldehyde (0–29.5 mmol) in enough chlorobenzene to make a total organic layer volume of 5 mL; 80 °C.

Subsequent to a rapid increase in reaction rate with formate ion concentration, between 0.5–2.5 M, the reaction rate leveled off (Figure 7). This kinetic behavior is analogous to that observed for the biphasic hydrogenation of benzaldehyde by the water-soluble TPPMS complex of Ru(II).<sup>19</sup>

The reaction rate was determined as a function of temperature over the range 55–90 °C (Figure 8) to afford an apparent activation energy of 23.9 kcal mol<sup>-1</sup>. Because of the aforementioned precautionary measures taken it is probably safe to assume that the kinetic control of this process is governed by the chemical reaction and not by physical phenomena.<sup>27</sup> The apparent activation energy ascertained herein is quite similar to that found of 23.4 kcal mol<sup>-1</sup> for the Ru(II)/TPPMS catalyzed hydrogenation of benzaldehyde with formate as the hydrogen source.<sup>19</sup> On the other hand it is markedly different than the  $E_a$  of 7 kcal mol<sup>-1</sup> reported for the Ru(II)/TPPTS catalyzed hydrogenation of 3-methyl-2-buten-1-ol with hydrogen.<sup>20</sup>

Reaction 3 catalyzed by complex 3 is greatly inhibited when carried out in the presence of a 10-fold excess of PTA or in excess carbon monoxide (see Table 8). The presence of less than four PTA ligands at the ruthenium center in the active catalyst is further substantiated by preparing a catalytic ruthenium species *in situ* from  $\text{Ru}(\text{H}_2\text{O})_6(\text{tos})_2$  and 1–6 equiv of PTA. The catalytic

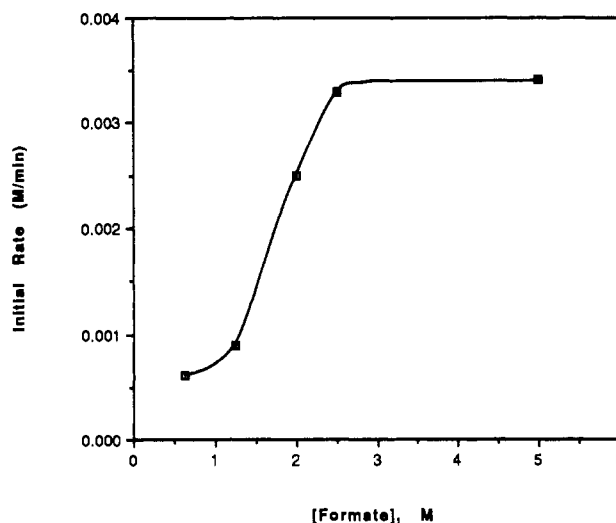


**Figure 7.** Dependence of the initial rate on the concentration of  $\text{HCOONa}$ . Conditions: 0.03 mmol  $\text{RuCl}_2(\text{PTA})_4$  in 5.0 mL of aqueous sodium formate (0.5–5.0 M); 4.92 mmol of benzaldehyde in 3.5 mL of chlorobenzene; 80 °C.

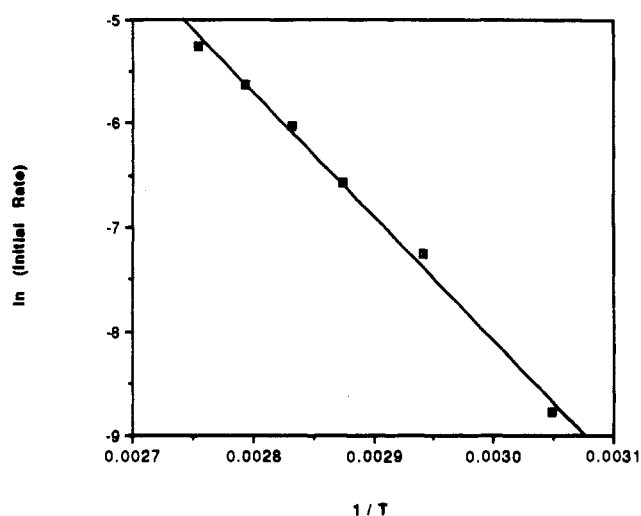


**Figure 8.** Arrhenius plot for the catalytic reduction of benzaldehyde by  $\text{RuCl}_2(\text{PTA})_4$ .

reduction of benzaldehyde was carried out as previously described, yielding the results shown in Figure 9. The maximum rate occurred when the metal:phosphine ratio was 1:3 and was inhibited by a phosphine:metal ratio  $\geq 4:1$ . Nevertheless, the rates differ by an order of magnitude for catalysts derived from complex 3 *vs*  $\text{Ru}(\text{H}_2\text{O})_6^{2+}$  in the presence of 4 equiv of PTA, suggesting that the electronic/steric factors about Ru(II) are different in the two instances.

After reduction of >50% of the substrate, the organic layer was removed and replaced with a fresh aliquot of benzaldehyde. It was found that the rate of catalytic reduction did not decrease after three consecutive cycles. Also noted during the recycling experiments was the production of a white, powdery material, which was shown to consist of sodium carbonate, sodium bicarbonate, and some coprecipitation of the hydrogen source, sodium formate.<sup>24</sup> Because of the complex equilibria exhibited by carbonate and bicarbonate in aqueous media, determination of which species is initially produced in the catalytic reaction was not possible.<sup>29</sup> During the course of the hydrogenation reaction there is a gradual, albeit slight, increase in the pH of the aqueous phase, from 8.59 to 9.18 (see Figure 10). This rise in pH is as

(29) Butler, J. N. *Carbon Dioxide Equilibria and Their Applications*, Addison-Wesley Publishing Co. 1982, p. 23.

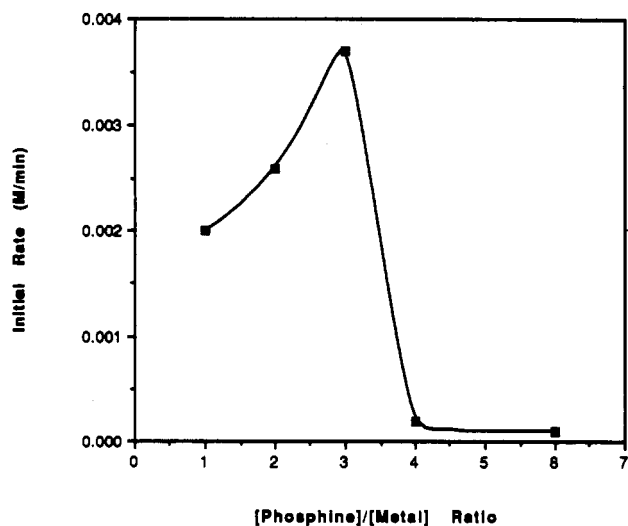


**Figure 9.** Dependence of the initial rate on the [P]/[Ru] ratio. Conditions: 0.03 mmol of  $\text{Ru}(\text{H}_2\text{O})_6\text{Tos}_2$  and free PTA (0.03–0.18 mmol) in 5.0 mL of 5 M aqueous sodium formate; 4.92 mmol of benzaldehyde in 3.5 mL of chlorobenzene; 80 °C.

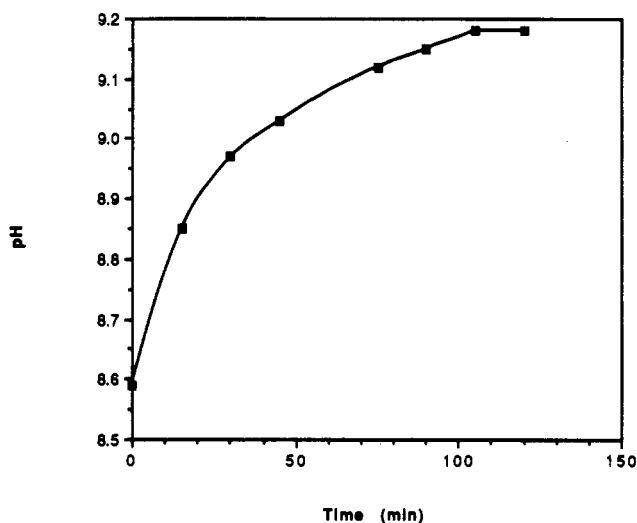
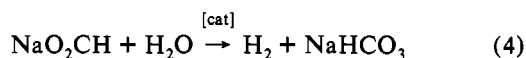


**Figure 10.** Time dependence of pH during the catalytic reduction of benzaldehyde by  $\text{RuCl}_2(\text{PTA})_4$ . Conditions: 0.06 mmol of  $\text{RuCl}_2(\text{PTA})_4$  in 5.0 mL of 5 M aqueous sodium formate; 4.92 mmol of benzaldehyde in 4.5 mL of chlorobenzene; 80 °C.

expected for a process which consumes protons (vide infra). However, in this range the rate of hydrogenation of benzaldehyde has been previously shown to be independent of pH.<sup>19</sup>

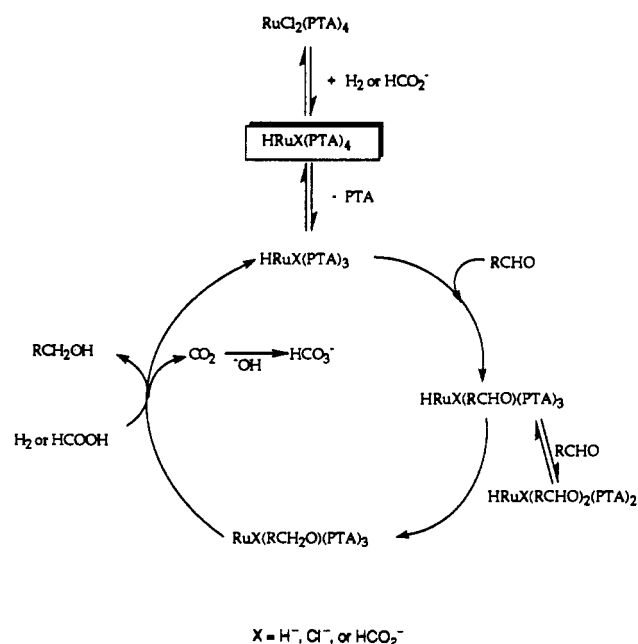
Furthermore, we have attempted to determine the source, and means of addition, of the hydrogen in this hydrogenation process. Specifically, does the hydrogen incorporated into the benzyl alcohol come from decomposition of sodium formate with water (eq 4) or via a direct transfer process. In order to address this



question a series of catalytic reductions were performed identical to those carried out in our kinetic investigation, but using solutions of (a)  $\text{D}_2\text{O}/\text{NaO}_2\text{CH}$ , (b)  $\text{H}_2\text{O}/\text{NaO}_2\text{CD}$ , and (c)  $\text{D}_2\text{O}/\text{NaO}_2\text{-CD}$ .<sup>27,30</sup> After allowing the catalysis to proceed for several hours, 10 mL of distilled  $\text{H}_2\text{O}$  was added to the reaction mixture. The resulting benzyl alcohol was isolated by column chromatography and analyzed by NMR and GC/MS techniques.

Mass spectral analysis demonstrated that the level of deuterium in the benzyl alcohol was considerably greater in experiment *b*

## Scheme 2



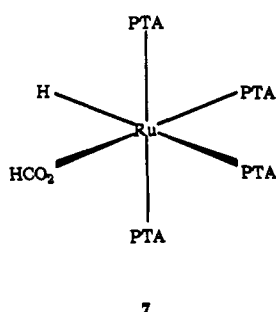
as compared with experiment *a*. Of course in experiment *c* essentially 100%  $\text{C}_6\text{H}_4\text{CDHOH}$  was afforded. This is as well seen in the  $^{13}\text{C}$  proton-decoupled NMR spectrum of benzyl alcohol where, in experiment *a* in addition to the singlet at 6.54 ppm corresponding to the benzyl carbon atom, a small triplet resulting from C–D coupling in  $\text{C}_6\text{H}_4\text{CDOH}$  is observed. On the other hand in experiment *b*, and as expected in experiment *c*, the triplet becomes the predominant resonance for the benzyl carbon atom. Hence, it is safe to conclude that the source of hydrogen is the formate ion, with some limited exchange with water occurring in the subsequently formed ruthenium hydride. This result is also consistent with the slow rate of hydrogenation observed when low concentrations of dihydrogen are employed as hydrogen source.

A catalytic cycle for the hydrogenation of benzaldehyde to benzyl alcohol employing complexes 3 or 4 in the presence of excess sodium formate which is consistent with our kinetic studies is illustrated in Scheme 2. That is, the process was found to be first order in catalyst and aldehyde concentration (at low aldehyde concentrations) and independent of formate at high formate concentration. It is assumed that the rate-determining step is the reaction of the metal-bound aldehyde with the metal hydride to afford the metal alkoxide intermediate. This cycle has several features in common with that described for the analogous ruthenium(II)/TPPMS system using  $\text{NaO}_2\text{CH}$  as hydrogen source with one notable exception.<sup>20</sup> The catalytic rate of reaction 4 involving the tetraphosphine  $\text{Ru}(\text{PTA})_4\text{Cl}_2$  catalyst precursor is greatly inhibited by excess phosphine ligand, whereas excess TPPMS is required in the  $\text{RuCl}_2(\text{TPPMS})_2$  process to have high conversions. An observation similar to that noted for the TPPMS process was observed for the  $\text{Ru}(\text{II})/\text{TPPTS}$  system using dihydrogen as the hydrogen source.<sup>20</sup> These observations have suggested that the catalytically active ruthenium species in these latter instances requires at least three phosphine ligands, a situation which the PTA system achieves by phosphine dissociation. Hence, the divergent behavior exhibited by the PTA and sulfonated phosphine catalysts is a manifestation of steric differences. That is, the small PTA ligand (cone angle  $102^\circ$ )<sup>14</sup> affords a stable  $\text{Ru}(\text{II})$  complex with four phosphine ligands, whereas the more bulky sulfonated phosphine (cone angles  $>165^\circ$ )<sup>12</sup> provide  $\text{Ru}(\text{II})$  derivatives with only two phosphine ligands. Part of the rate enhancement seen in the presence of excess sulfonated phosphine is probably attributable to the surface-active properties of these particular water-soluble phosphines, which would result in a more

(30) Bar, R.; Sasson, Y.; Blum, J. *Org. Magn. Reson.* 1984, 22, 565.



rapid migration of the aldehyde into the aqueous catalytic phase. This phenomenon may account for the somewhat faster hydrogenation rates observed for the TPPTM and TPPTS ruthenium(II) catalysts as compared with the PTA system reported upon herein which are  $\sim 30$  times slower. The boxed species in Scheme 2, which is formed in the catalyst pretreatment period prior to addition of aldehyde, is most likely a ruthenium(II) formate-hydride complex as evidenced by  $^1\text{H}$  and  $^{31}\text{P}$  NMR spectroscopy. To be specific, treatment of  $\text{RuCl}_2(\text{PTA})_4$  with  $\text{NaHCO}_2$  at  $60^\circ\text{C}$  for a few minutes resulted in a color change of the solution from orange-yellow to bright light yellow with concomitant formation of  $\text{CO}_2$  bubbles. The  $^{31}\text{P}$  NMR spectrum of the resultant solution consisted of a doublet of triplets centered at  $-30.1$  ppm, while the proton NMR spectrum showed a hydride signal at  $-18.4$  ppm. There was no  $^{31}\text{P}$  resonance corresponding to free PTA in solution. Because of the large excess of free sodium formate present in the reaction solution it was not possible to identify a signal due to metal bound formate. Hence, we have tentatively assigned X in the cycle in Scheme 2 as  $\text{HCO}_2^-$ . That is, the boxed species is derivative 7.



Although alkoxide intermediates resulting from aldehyde insertion into the metal-hydride bond are not directly observed in this instance, such species have been noted from the reactions of anionic group 6 metal hydrides with aldehydes and ketones.<sup>31-33</sup> Furthermore, evidence for their existence has been presented in homogeneous ruthenium(II)-catalyzed hydrogenation of aldehydes processes.<sup>34-37</sup> The inhibitory effect of large excesses of

aldehydes via formation of bis(aldehyde) derivatives has previously been reported.<sup>19,27</sup> Further studies in our laboratory are directed at obtaining additional, more definitive evidence for the catalytic cycle presented in Scheme 2.

### Concluding Remarks

The ruthenium(II) derivative  $\text{RuCl}_2(\text{PTA})_4$  is shown to be an effective catalyst for the regioselective hydrogenation of aldehydes to alcohols in the presence of aqueous solutions of sodium formate. Although the reaction rate is somewhat slower than the analogous process involving the sulfonated triphenylphosphine species, the process reported upon herein does not require the presence of excess phosphine ligand as the former process does. Hence, its small steric requirements, coupled with its enhanced basicity, makes the water-soluble, air-stable phosphine 1,3,5-triaza-7-phosphaadamantane an attractive alternative to sulfonated phosphine for purposes of organometallic catalysis in aqueous or biphasic solutions.

**Acknowledgment.** The financial support of this research by the National Science Foundation (Grants CHE91-19737 and INT90-08227) and Hungarian Academy of Science (Grant 30.008/134/90) and the Hungarian National Research Foundation (Grant OTKA 1699) is greatly appreciated. We are as well appreciative of the lucid comments of our reviewers.

**Supplementary Material Available:** Complete listings of bond lengths, bond angles, anisotropic displacement parameters, and H-atom coordinates for complexes 3-5 (9 pages). Ordering information is given on any current masthead page.

- (31) Gaus, P. L.; Kao, S. C.; Youngdahl, K.; Darensbourg, M. Y. *J. Am. Chem. Soc.* **1985**, *107*, 3428.
- (32) Kao, S. C.; Gaus, P. L.; Youngdahl, K.; Darensbourg, M. Y. *Organometallics* **1984**, *3*, 1601.
- (33) Tooley, P. A.; Ovalles, C.; Kao, S. C.; Darensbourg, D. J.; Darensbourg, M. Y. *J. Am. Chem. Soc.* **1986**, *108*, 5465.
- (34) Grey, R. A.; Pez, G. P.; Wallo, A.; Corsi, J. *Ann. N. Y. Acad. Sci.* **1983**, *415*, 235.
- (35) Halpern, J. *Ann. N. Y. Acad. Sci.* **1983**, *415*, 244.
- (36) Sanchez-Delgado, R. A.; Andriollo, A.; DeOchoa, O. L.; Suarez, T.; Valencia, N. *J. Organomet. Chem.* **1981**, *209*, 77.
- (37) Sanchez-Delgado, R. A.; Valencia, N.; Marquez-Silva, R. -L.; Andriollo, A.; Medina, M. *Inorg. Chem.* **1986**, *25*, 1106.